Volume 24, No 2 | International Journal of Radiation Research, April 2026

Integrating MR imaging and clinical features to differentiate uterine carcinosarcoma from endometrial carcinoma

Z. Huang[1], Y. Jiang[1], L. Wan[2], W. Chen[1], J. Zhao[1*]

[1]*Radiology Department, The Second Affiliated Hospital of Guangzhou University of Chinese Medicine, Guangzhou, 510120, Guangdong, China*

[2]*Guangzhou Cadre and Talent Health Management Center, Guangzhou, 510530, Guangdong, China*

► ***Original article***

Corresponding author:
Iaxin Zhao, M.Sc.,
E-mail: *453606904@qq.com*

Received: December 2024
Final revised: June 2025
Accepted: July 2025

Int. J. Radiat. Res., April 2026; 24(2): 473-480

DOI: 10.61186/ijrr.24.2.25

Keywords: *Uterine carcinosarcoma, endometrial neoplasms, magnetic resonance imaging, diffusion magnetic resonance imaging, gynecological malignancy.*

ABSTRACT

Background: This study aimed to investigate the clinical and MRI features of uterine carcinosarcoma (UCS) and endometrial carcinoma (EC), and to explore how integrating these characteristics could help distinguish UCS from EC. ***Materials and Methods:*** A total of 33 UCS patients and 114 EC patients were included in this study. Mann-Whitney U test was used to compare clinical-pathological characteristics and MR features between UCS and EC groups. Univariate and multivariate logistic regression analyses were conducted to identify the factors differentiating UCS from EC. Receiver operating characteristic (ROC) curve and area under the curve (AUC) were used to evaluate diagnostic ability to distinguish UCS from EC. ***Results:*** UCS patients exhibited higher median age and elevated levels of carbohydrate antigen12-5 (CA 12-5) than EC patients. Compared to EC, UCS showed a greater propensity for ill-defined boundary, tumor prolapse, heterogeneous T2WI signals, hemorrhage, cystic degeneration, and more advanced stage than EC. The tumor size, anterior-posterior (AP) dimension, the ratio of the endometrial thickness (ET) to AP, and apparent diffusion coefficient (ADC) value of UCS were significantly larger than those of EC. Multivariate analysis identified independent factors for differentiating UCS from EC, including ill-defined tumor boundary, heterogenous T2WI signal intensity, heterogenous enhancement pattern, larger tumor volume, greater AP dimension, and higher ADC value. The AUC of the multivariate analysis for differentiating UCS from EC was 0.935, with 87.88% sensitivity and 94.74% specificity. ***Conclusion:*** Combining clinical characteristics with MRI features may significantly enhance the differentiation of UCS from EC.

INTRODUCTION

Uterine carcinosarcoma (UCS) is a very rare and aggressive malignant tumor. Histologically, this biphasic neoplasm is characterized by the presence of both carcinomatous and sarcomatous elements originating from a single malignant clone. Recent studies suggest that UCS may be classified as a subtype of high-grade carcinoma [1]. UCS contains frequent mutations in TP53 and is characterized by aggressiveness [2]. Moreover, UCS demonstrate a significant and broad variation of epithelial to mesenchymal transition scores, which correlated with its metastatic potential [3]. UCS represents a formidable diagnostic challenge in gynecologic oncology. It accounts for less than 5% of uterine tumors yet carries a disproportionately poor prognosis, with only 35% of patients surviving five years post-diagnosis [4, 5]. Its biphasic histology and nonspecific clinical presentation, frequently leads to preoperative misclassification. This diagnostic uncertainty has dire consequences, as even early-stage UCS demonstrates a 45% recurrence rate and 50% disease-related mortality within five years [6].

The clinical manifestations of UCS lack specificity and often overlap with those of endometrial carcinoma (EC) or uterine sarcomas, making identification challenging based solely on clinical presentations. Given the aggressive nature of UCS and its high risk of recurrence and metastasis, more extensive surgical procedures, such as pelvic and para-aortic lymphadenectomy, are typically recommended [6]. Additionally, adjuvant therapy is often advocated to improve outcomes in patients with UCS [7]. The critical need for improved diagnostic tools is underscored by the stark management divergence between UCS and EC, as optimal surgical and adjuvant approaches differ substantially.

While magnetic resonance imaging (MRI) serves as the cornerstone for evaluating uterine malignancies, conventional diagnostic approaches remain imperfect. Existing studies have identified characteristic UCS features such as heterogeneous T2 signal, tumor prolapse, and restricted diffusion on diffusion weighted imaging (DWI), yet these findings often overlap with high-grade EC [8-13]. Notably, conflicting reports regarding apparent diffusion coefficient (ADC) values - with some studies showing similarity to low-grade EC and others demonstrating significant differences - highlight fundamental gaps in

[DOI: 10.61186/ijrr.24.2.25]

our understanding. These diagnostic ambiguities persist despite advances in molecular characterization, including the recognition of frequent TP53 mutations and epithelial-mesenchymal transition signatures in UCS. The absence of a robust, integrated diagnostic framework combining clinical, imaging, and molecular markers represents a critical unmet need in the field.

Magnetic resonance imaging (MRI) serves as a valuable modality in the management of uterine malignancies. Conventional MR allows for comprehensive assessment of lesion identification, characterization, myometrial invasion, and lymph node involvement. Diffusion-weighted imaging (DWI) can detect microscopic changes at the molecular level, providing information about cellularity and tissue microstructure. Previous studies have indicated that characteristic MR features of UCS, such as a prominent polypoid mass causing endocervical canal dilation, heterogenous hyperintensity on T2WI, iso-intensity on T1WI, presence of tumor hemorrhage and prolonged enhancement [8-11]. On DWI, UCS demonstrated restricted diffusion attributed to its elevated cellularity and compact cytoarchitectonics, manifesting as hyperintensity on DWI and hypointensity on apparent diffusion coefficient (ADC) map [12, 13]. DWI is also helpful in assessing the extent of deep myometrial or cervical stromal invasion in UCS [14]. Despite these findings, differentiation between UCS and EC can be challenging due to overlapping MR imaging characteristics. Therefore, this study aimed to investigate the clinical and MRI characteristics of UCS and EC, and to explore the potential utility of integrating these features for differentiation UCS from EC.

By systematically analyzing the largest UCS cohort to date (n=33) against 114 EC cases, we developed a novel diagnostic model integrating clinical parameters with advanced MRI biomarkers. The aim to this study is to provide a comprehensive comparison of clinical and MRI features between UCS and EC, integrating quantitative imaging biomarkers with qualitative assessments to enhance preoperative differentiation.

MATERIALS AND METHODS

Patients

This study was approved by the local ethics committee's institutional review board. A retrospective review of the database was conducted for consecutive patients with UCS and EC from January 2011 to May 2023 was performed. The inclusion criteria for the study were: 1) surgical confirmation of UCS and EC via pathological assessment. 2) the presence of complete clinical and MR data. The criteria for exclusion included: 1) additional therapeutic intervention (chemotherapy, radiotherapy, or targeted therapy) before surgery; 2) poor MR image quality or severe artifact; 3) incomplete clinical information.

Eventually, 33 patients with pathological confirmed UCS and 114 patients with pathological confirmed EC were enrolled. The patient selection flowchart is illustrated in figure 1.

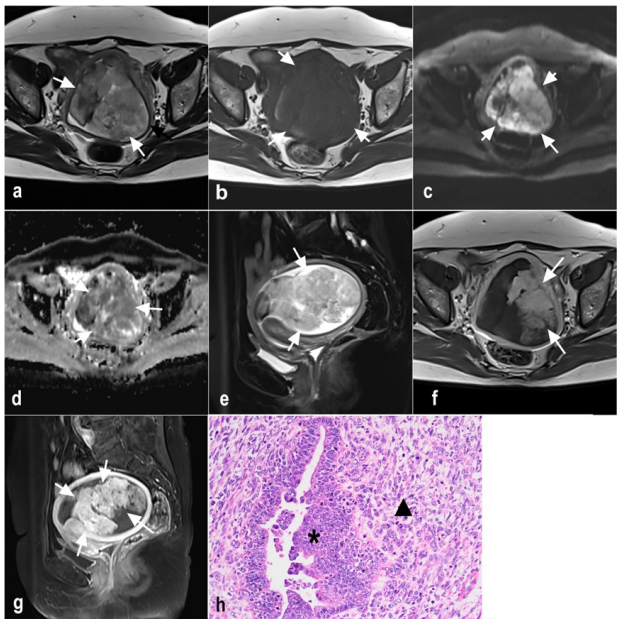

Figure 1. A 67-year-old woman was diagnosed with FIGO IIIc UCS. MR demonstrated a large mass within the uterus, displaying heterogeneous signal intensity on T2WI (white arrow, **a** and **e**). The lesion demonstrates hyperintensity on T1WI (white arrow, **b**) attributable to hemorrhage, hyperintense on DWI (white arrow, **c**) and hypointense on ADC map (white arrow, **d**). The tumor exhibited early intense enhancement in its solid portion (white arrow, **f** and **g**). Corresponding H&E-stained histopathology (400×, **h**) revealed that the tumor was a mix of high-grade serous carcinoma (black star) and rhabdomyosarcoma (black rectangle).

Clinical features

The clinical features were collected from Hospitalization Information System, which included age, postmenopausal, vaginal bleeding, and levels of blood tumor markers such as carbohydrate antigen 19-9 (CA19-9), carbohydrate antigen 12-5, (CA12-5), carbohydrate antigen 15-3 (CA15-3), alpha-fetoprotein (AFP), carcinoembryonic antigen (CEA).

Histopathology evaluation

Histological sections of the primary tumor and lymph nodes were fixed in formalin, cut into 4 μm sections, and stained with hematoxylin and eosin (Beiant,China). Histological assessments were performed by an experienced pathologist. All the tumors were classified histologically based on criteria set by World Health Organization and the International Federation of Gynecology and Obstetrics (FIGO) 2009 system. For both EC and USC, the evaluation includes lymph node metastasis and lymphovascular space invasion. The histological

[DOI: 10.61186/ijrr.24.2.25]

grading criteria for EC are defined as follows: 1) Grade 1: less or equal 5% solid architecture, minimal cellular atypia, low mitotic activity, high degree of resemblance to normal cells, and favorable prognosis. 2) Grade 2: 6%–50% solid architecture, moderate cellular atypia, intermediate mitotic activity, malignancy level intermediate between Grade 1 and Grade 3, and moderate prognosis. 3) Grade 3: more than 50% solid architecture, marked cellular atypia, high mitotic activity, significant morphological deviation from normal cells, high-grade malignancy, and relatively poor prognosis. For USC, tumor histological components are additionally evaluated.

MR imaging protocol

MR imaging was performed with a 1.5 T scanner (Magnetom Avanto, Siemens, Erlangen, Germany) and a 3.0 T scanner (Magnetom Verio, Siemens, Erlangen, Germany). All images were obtained with a phased array body coil. The imaging protocol encompassed T2-weighted imaging (T2WI), DWI, and both plain and contrast-enhanced T1-weighted imaging (T1WI), which were acquired in the axial, coronal, and sagittal planes. Contrast- enhanced T1WI was conducted in the axial, sagittal and coronal planes after intravenous administration of 2 mmol/kg of gadopentetate dimeglumine (Magnevist, Bayer Healthcare, Germany). The ADC mapping images were reconstructed based on the two image sets of different b values. The magnetic resonance scanning parameters are summarized in table 1.

Table 1. MR scanning protocol.

	Siemens Avanto 1.5T				Siemens Verio 3.0T			
	T1WI/CE T1WI	T1WI FS	T2WI/T2 FS	DWI	T1WI/CE T1WI	T1WI FS	T2WI/T2 FS	DWI
MR Sequence	Spin echo	Turbo spin echo	Turbo Spin Echo	Echo Planar	Spin echo	Turbo spin echo	Fast Spin Echo	Echo Planar
Repetition time/Echo Time (ms)	429/11	707/11	5090/72	5700/83	819/11	707/11	4000/84	5900/83
Echo Train Length	2	2	14	1	4	2	28	1
Flip Angle (°)	180	180	150	90	140	180	90	90
Slice thickness (mm)	5	5	5	5	5mm	5	5	5mm
(Pixel) Bandwidth	186	186	161	1250	260	186	260	1628
Matrix	320×320	320×240	320×320	256×256	256×256	320×240	256×256	256×256
Field of View (mm)	320	370	370	260×	350	370	280	280

CE, contrast enhanced; DWI, diffusion weighted imaging; FS, fat suppression

MR imaging analysis

All MR images were evaluated retrospectively by two radiologists who were unaware of the clinical-pathologic features. The MRI assessment included the qualitative and quantitative features. Qualitative MRI features were evaluated as follows:1) tumor morphology: tumor boundary, classified as either well-defined or poorly defined; tumor prolapse, defined as protrusion of the tumor through the cervical os (present/absent). 2) tumor composition: hemorrhage, identified by high signal intensity on T1WI and variable signal intensity on T2WI (depending on hemorrhage age/stage); cystic degeneration or necrosis, characterized by T2WI hyperintense regions without post-contrast enhancement. 3) contrast enhancement: the enhancement pattern, classified as homogeneous or heterogeneous; the degree of enhancement, graded as mild, moderate or marked (relative to myometrial enhancement). 4) signal characteristics: assessed as homogeneous or heterogeneous. Quantitative analysis included tumor size metrics and diffusion metrics: 1) tumor size metrics: measurement tumor volume, tumor size in anterior-posterior (AP) direction on the sagittal T2WI, the ratio of the endometrial thickness (ET) to AP dimension (ET/AP). 2) diffusion metrics: mean ADC values. The ADC was measured using two different b value: 0 and 800 s/mm^2 according to the following formula: ADC = -ln (S_1/S_0)]/(b1-b0), where S0 is signal intensity for b = 0 and S_1 is the signal intensity for b = 800 s/mm^2.

Statistics analysis

The consistency of the measurements was evaluated using Cohen's Kappa test or the inter-class correlation coefficient (ICC), with scores above 0.80 indicating excellent agreement. Comparisons between UCS and EC were conducted using the two-sample t-test (normally distributed data) or the Mann -Whitney U test (non-parametric data). Univariate and multivariate logistic regression analyses were performed to identify distinguishing factors between UCS and EC, with odds ratios (OR) and 95% confidence intervals (CI) calculated. Hosmer-Lemeshow test was performed to assess goodness-of-fit. Receiver operating characteristic (ROC) curve analysis was conducted to assess diagnostic capability of models in differentiating UCS from EC. The ROC curves were compared using DeLong test to determine the difference between the area under the curve (AUC). SPSS, version 20 (IBM, Armonk, New York, USA) and MedCalc, version 19.1.2 (MedCalc Software, Ostend, Belgium) were used for statistical analysis, with a *p*-value of less than 0.05 considered as statistically significant.

RESULTS

Patient demographic data

Eventually, 33 UCS patients and 114 EC patients were respectively enrolled for analysis. The demographic data of the patients are presented in

[DOI: 10.61186/ijrr.24.2.25]

table 2. The median age of patients with UCS was significantly higher than that of EC patients, at 59.91 years compared to 54.28 years (p=0.004). Additionally, 63.6% of patients with UCS exhibited elevated levels of CA 12-5, which was significantly greater than the 43.0% observed in EC patients (p=0.036). However, no statistically significant differences were found between UCS and EC groups regarding postmenopausal status, vaginal bleeding, or levels of abnormal AFP, CEA, CA19-9, and CA15-3.

Table 2. Clinical and histological characteristics of UCS and EC.

	UCS (n=33)	EC (n=114)	Kappa value	P value
Age (year)	59.91±10.47	54.28±9,59		0.004
Postmenopausal				
Yes	28 (84.8%)	79 (69.3%)	0.032	0.118
No	5 (15.2%)	35 (30.7%)		
Vaginal bleeding			0.026	
Yes	25 (75.8%)	72 (63.2%)		0.214
No	8 (24.2%)	42 (36.8%)		
AFP				
Abnormal (>7ng/ml)	0	11 (9.6%)	-0.017	0.064
Normal (≤7ng/ml)	33 (100.0%)	103 (90.4%)		
CEA				
Abnormal (>5ng/ml)	3 (9.1%)	16 (14.0%)	-0.009	0.567
Normal (≤5ng/ml)	30 (90.9%)	98 (86.0%)		
CA 12-5 Abnormal (>35U/ml)	21 (63.6%)	49 (43.0%)	0.040	0.036
Normal (≤35U/ml)	12 (36.4%)	65 (57.0%)		
CA 19-9				
Abnormal (>37U/ml)	4 (12.1%)	26 (22.8%)	-0.019	0.180
Normal (≤37U/ml)	29 (87.9%)	88 (86.7%)		
CA 15-3				
Abnormal (>30U/ml)	8 (24.2%)	15 (13.2%)	0.020	0.171
Normal (≤30U/ml)	25 (75.8%)	99 (86.8%)		
FIGO Stage				
Ia	9 (27.3%)	58 (50.9%)	-0.077	0.002
Ib	12 (36.4%)	36 (31.6%)		
II	6 (18.2%)	17 (14.9%)		
III	3 (9.1%)	3 (2.6%)		
IV	3 (9.1%)	0		
Lymphatic metastasis				
Negative	28 (84.8%)	111 (97.4%)	0.022	0.015
Positive	5 (15.2%)	3 (2.6%)		
LVSI				
No	19 (57.6%)	65 (57.0%)	-0.001	0.954
Yes	14 (42.4%)	49 (43.0%)		

AFP, alpha fetoprotein; CA 12-5, carbohydrate antigen 12-5; CA 19-9, carbohydrate antigen 19-9; CA 15-3, carbohydrate antigen 15-3; CEA, carcinoembryonic antigen; FIGO, International Federation of Gynecology and Obstetrics; LVSI, lymphovascular space invasion.

Pathologic features

All UCS specimens in this study presented showed diverse histological features, including epithelial cells and spindle cells of varying sizes and shapes, undergoing pathologic mitosis. The presence of various sarcomatous elements, such as endometrial stromal sarcoma, osteosarcoma, fibrosarcoma and chondrosarcoma, was noted. Based on the sarcomatous components, the specimens were categorized into homologous (10 cases) and heterogenous types (16 cases), with 7 cases unclassifiable. In cases of EC, 9 cases (7.9%) were classified as Grade 1, 89 cases (78.1%) as Grade 2, and 16 cases (14.0%) as grade 3.

MR features

Kappa and the ICC statistic results showed excellent agreement for MR features evaluation (Kappa score range from 0.80 to 0.90, ICC value range from 0.83 to 0.97, all p<0.001, table 3).

Table 3. Interobserver agreement evaluation.

MR Features	Kappa value/ ICC (95% CI)
Boundary	0.82 (0.74-0.95)
Tumor Prolapse	0.80 (0.66- 0.99)
Hemorrhage	0.83 (0.69-0.88)
Cystic degeneration	0.85 (0.78-0.96)
Enhanced pattern	0.88 (0.76-1.00)
Enhanced Degree	0.84 (0.81-0.87)
T2WI SI	0.90 (0.86- 0.93)
Tumor volume (cm^3)	0.83 (0.72-0.91)
AP (cm)	0.86 (0.81-0.91)
ET/AP	0.87 (0.81-0.91)
mean ADC value ($\times10^{-3}mm^2/s$)	0.84 (0.72-0.91)

ADC, apparent diffusion coefficient; AP,anterior-posterior; ET/AP, endometrial thickness/anterior-posterior dimension; SI, signal intensity.

Table 4 presents a comparison of MR findings related to tumor characteristics, including tumor boundary, hemorrhage, cystic degeneration, T2WI signal intensity, enhancement pattern, tumor prolapse, tumor size, AP dimension and ET/AP ratio.

Table 4. MR features of UCS and EC.

MR Features	UCS	EC	*Kappa* or *F* value	*P* value
Boundary				
Well-defined	18 (54.5%)	85 (74.6%)	0.037	0.027
ill-defined	15 (45.5%)	29 (25.4%)		
Hemorrhage				
Absent	19 (57.6%)	95 (83.3%)	0.047	0.002
Present	14 (42.4%)	19 (16.7%)		
Cystic degeneration				
No	20 (60.6%)	102 (89.5)	0.052	<0.001
Yes	13 (57.6%)	12 (10.5%)		
T2WI SI				
Homogenous	3 (9.1%)	79 (69.3%)	0.020	<0.001
Heterogenous	30 (90.9%)	35 (30.7%)		
Enhanced pattern				
Homogenous	11 (33.3%)	91 (79.8%)	0.087	<0.001
Heterogenous	22 (66.7%)	23 (20.2%)		
Enhanced Degree				
Mild	9 (27.3%)	40 (35.1%)	0.033	0.604
Moderate	14 (42.4%)	68 (59.6%)		
marked	10 (30.3%)	6 (5.3%)		
Tumor Prolapse				
No	16 (48.5%)	94 (82.5%)	0.063	<0.001
Yes	17 (51.5%)	20 (17.5%)		
Tumor size				
Tumor volume (cm^3)	52.54 (72.35)	32.45 (16.93)	-3.941	<0.001
AP (cm)	4.02 (1.83)	3.04 (1.80)	-3.102	0.002
ET/AP ratio	0.632 (0.182)	0.452 (0.271)	-2.654	0.008
ADC value ($\times10^{-3}$ mm^2/s)	1.092 (0.148)	1.040 (0.240)	-2.604	0.009

ADC, apparent diffusion coefficient; AP, anterior-posterior; ET/AP,endometrial thickness/anterior-posterior dimension; SI,signal intensity.

[DOI: 10.61186/ijrr.24.2.25]

On MRI, an ill-defined boundary was observed in 45.5% of UCS cases, which was significantly higher that observed in EC (*p=0.027*). Approximately half of UCS cases (51.5%, 17/33) exhibited tumor prolapse into the endocervical canal, a higher frequency than observed in EC. In comparison to EC, UCS exhibited a greater propensity for heterogeneous T2WI signals indicative of tumor (90.9% vs 30.7%, $p<0.001$), hemorrhage (42.4% vs 16.7%, $p=0.002$), or cystic degeneration (57.6% vs 10.5%, $p<0.001$) within the tumor.

In UCS, a heterogenous enhancement pattern was observed in 66.7% (22/33) of cases, with the remaining 33.3% (11/33) exhibiting a homogenous pattern. Most UCS cases showed a moderate (42.4%) or marked (30.3%) degree of enhancement compared to normal myometrium following the administration of contrast agents. However, this difference was not statistically significant when compared to EC ($p=0.604$). Approximately 18.2% (6/33) of UCS cases were diagnosed at FIGO stage II, and another18.2 % were diagnosed at advanced stages (FIGO stage III and IV), which was a higher proportion than that observed in EC ($p=0.002$). The tumor size, AP dimension, and ET/AP ratio of UCS were significantly larger than those of EC ($p<0.001$, $p=0.002$, and $p=0.008$, respectively). Furthermore, the mean ADC value of UCS was significantly higher than that of EC ($p=0.009$). The representative MR features of UCS and EC are illustrated in figure 1 and 2, respectively.

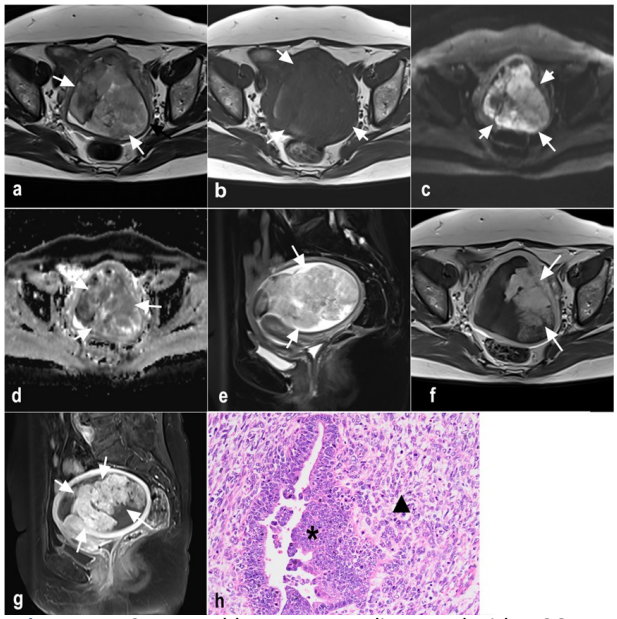

Figure 1. A 67-year-old woman was diagnosed with FIGO IIIc UCS. MR demonstrated a large mass within the uterus, displaying heterogeneous signal intensity on T2WI (white arrow, **a** and **e**). The lesion demonstrates hyperintensity on T1WI (white arrow, **b**) attributable to hemorrhage, hyperintense on DWI (white arrow, **c**) and hypointense on ADC map (white arrow, **d**). The tumor exhibited early intense enhancement in its solid portion (white arrow, **f** and **g**). Corresponding H&E-stained histopathology (400×, **h**) revealed that the tumor was a mix of high-grade serous carcinoma (black star) and rhabdomyosarcoma (black rectangle).

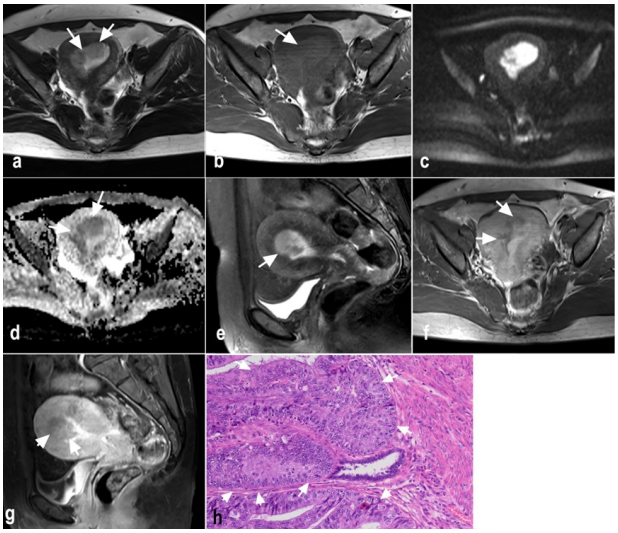

Figure 2. A 45-year-old woman with a FIGO Ia EC. The tumor demonstrated a intermediate signal intensity on T2WI (white arrow, **a**), and iso-intensity on T1WI (white arrow, **b**), with diffusion restriction on DWI (white arrow, **c** and **d**). There is invasion of the myometrium, extending to less than 50% of the myometrial thickness (white arrow, **e**). The post-contrast image demonstrates the typical bright enhancement of the myometrium with intermediate enhancement of the tumor (white arrow, **f** and **g**). Corresponding H&E-stained histopathology (400×, **h**) revealed a moderate differentiated endometrial adenocarcinoma (white arrow).

Table 5 showed the univariate analysis of factors and diagnostic performance in differentiating UCS from EC. Univariate analysis demonstrated that the AUCs for elevated CA12-5, tumor boundary, hemorrhage, cystic degeneration, T2WI SI, enhancement pattern, tumor FIGO stage, tumor prolapse, tumor volume, AP dimension, ET/AP ratio and ADC value were 0.603, 0.600, 0.629, 0.644, 0.654, 0.671, 0.656, 0.670, 0.726, 0.678, 0.652, and 0.649, respectively (figure 3a).

Multivariate analysis identified several independent factors for differentiating UCS from EC (table 6). These factors included ill-defined tumor boundary (OR 1.235, 95% CI 0.325- 4.493, $p=0.036$), heterogenous T2WI signal intensity of tumor (OR 4.552, 95% CI 1.093- 18.953, $p=0.037$), heterogenous enhancement pattern (OR 4.771, 95% CI 1.240- 17.893, $p=0.023$), larger tumor volume (OR 0.959, 95% CI 0.929- 0.989, $p=0.008$), greater AP dimension (OR 0.337, 95% CI 0.176- 0.643, $p=0.001$), and higher ADC value (OR 0.004, 95% CI 0.000- 0.198, $p=0.006$). The forest plots illustrated the impact of the dependent variables in the multiple logistic regression analysis (figure 4). The Hosmer–Lemeshow test indicated that the model met the criteria for an acceptable fit (Chi-square= 9.061, DF=8, $p=0.260$). The AUC of the multivariate analysis for differentiating UCS from EC was 0.935, with 87.88% sensitivity and 94.74% specificity ($p<0.001$) (figure 3b).

[DOI: 10.61186/ijrr.24.2.25]

Table 5. Univariate analysis of factors and diagnostic performance in differentiating UCS from EC.

Parameter	Odds Ratio (95% CI)	*P* value	AUC (95% CI)	Sensitivity	Specificity	*P* value
CA12-5	2.321 (1.043-5.168)	0.039	0.603 (0.494-0.712)	63.64%	57.02%	0.003
Boundary	2.443 (1.093-5.460)	0.030	0.600 (0.487-0.714)	45.45%	74.56%	0.039
Hemorrhage	3.684 (1.578-8.603)	0.003	0.629 (0.514-0.744)	42.42%	83.33%	0.024
Cystic degeneration	5.525 (2.203-13.856)	<0.001	0.644 (0.528-0.761)	39.39%	89.47%	0.012
T2WI SI	3.561 (1.571-8.074)	0.002	0.654 (0.547-0.760)	66.67%	64.04%	0.007
Enhancement Pattern	4.162 (1.827-9.480)	0.001	0.671 (0.565-0.777)	66.67%	67.54%	0.003
Tumor prolapse	4.994 (2.164-11.522)	<0.001	0.670 (0.558-0.782)	51.51%	82.46%	0.003
FIGO Stage	--	0.999	0.656 (0.546-0.766)	72.73%	50.88%	0.006
Tumor Volume (cm^3)	0.962 (0.946-0.979)	<0.001	0.726 (0.612-0.839)	48.48%	93.86%	<0.001
AP (cm)	0.602 (0.430-0.842)	0.003	0.678 (0.575-0.781)	48.48%	82.46%	0.002
ET/AP ratio	0.073 (0.008-0.683)	0.022	0.652 (0.548-0.756)	81.82%	60.53%	0.008
ADC value ($\times10^{-3}mm^2/s$)	0.041 (0.003-0.497)	0.012	0.649 (0.573-0.773)	81.82%	46.49%	0.004

ADC, apparent diffusion coefficient; AP, anterior-posterior; CA12-5, carbohydrate antigen 12-5; ET/AP, endometrial thickness/anterior-posterior dimension; FIGO,International Federation of Gynecology and Obstetrics; SI, signal intensity.

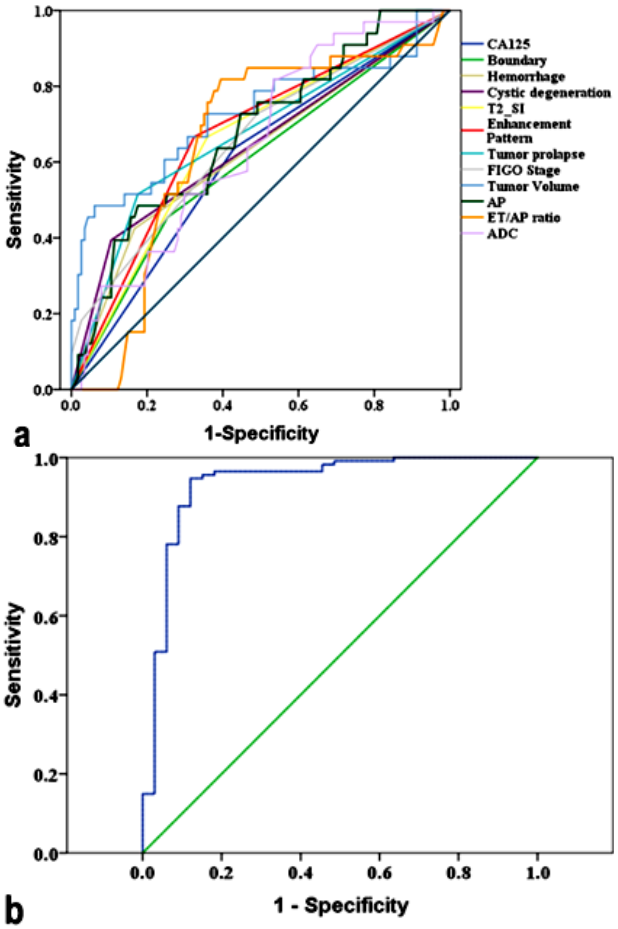

Figure 3. Receiver operating characteristic curves of univariate analysis **(a)** and multivariate analysis **(b)** for differentiating UCS from EC. Details of the area under the curves of each index are shown in the results section.

Table 6. Multivariate analysis of factors in differentiating UCS from EC.

Parameter	Odds Ratio (95% CI)	*P* value
CA12-5	1.235 (0.325-4.693)	0.757
Boundary	4.456 (1.102-18.028)	0.036
Hemorrhage	1.124 (0.141-8.982)	0.913
Cystic degeneration	5.139 (0.638-41.411)	0.124
T2WI SI	4.552 (1.093-18.953)	0.037
Enhancement Pattern	4.711 (1.240-17.893)	0.023
Tumor prolapse	1.894 (0.389-9.222)	0.429
FIGO Stage	--	0.697
Tumor Volume (cm^3)	0.959 (0.929-0.989)	0.008
AP (cm)	0.337 (0.176-0.643)	0.001
ET/AP ratio	0.480 (0.008-28.183)	0.724
ADC value ($\times10^{-3}mm^2/s$)	0.004 (0.000-0.198)	0.006

ADC, apparent diffusion coefficient; AP, anterior-posterior; CA12-5, carbohydrate antigen 12-5; ET/AP, endometrial thickness/anterior-posterior dimension; FIGO, International Federation of Gynecology and Obstetrics; SI, Signal intensity.

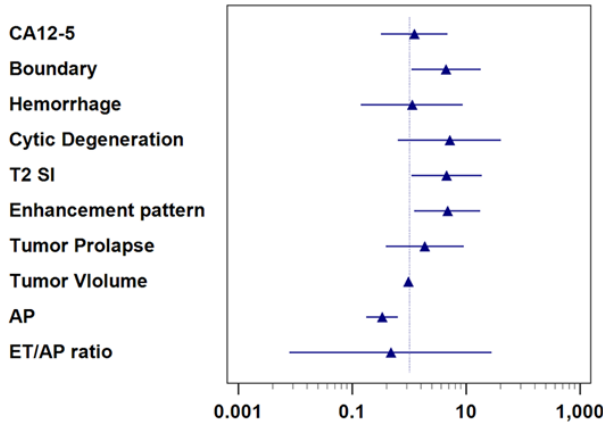

Figure 4. The forest plots illustrated the impact of the dependent variables in the multiple logistic regression analysis.

DISCUSSION

By systematically analyzing the largest UCS cohort to date (n=33) against 114 EC cases, we developed a novel diagnostic model integrating clinical parameters with advanced MRI biomarkers. To our knowledge, this is the first study to integrate AP dimension, ET/AP ratio, and ADC into a multivariate model for UCS and EC differentiation. The resulting model achieves exceptional diagnostic performance (AUC 0.935), surpassing existing methods. Our key findings suggest that UCS typically presents as a large, heterogeneous mass with ill-defined borders, frequent tumor prolapse, and higher ADC values compared to EC. These features align with prior studies highlighting the aggressive nature and complex histology of UCS [15, 16]. These findings not only enhance preoperative diagnostic accuracy but also offer immediate clinical utility for surgical planning and personalized therapeutic strategy.

UCS is a highly aggressive malignancy characterized by its biphasic histology, combining

[DOI: 10.61186/ijrr.24.2.25]

malignant epithelial and mesenchymal components. While its clinical presentation often overlaps with EC, our study identified key distinctions, including older age and elevated CA12-5 levels in UCS patients-factors previously linked to advanced disease and poor prognosis [18-20]. Notably, UCS was more frequently diagnosed at advanced FIGO stages, with 18.2% of cases showing distant metastasis. These findings reinforce the need for early and accurate diagnostic tools to guide aggressive therapeutic strategies.

MRI serves as a critical modality for evaluating uterine malignancies, offering insights into tumor morphology and biological behavior. In our cohort, UCS typically manifested as a large, well-defined mass with heterogeneous T2WI signal intensity, frequent prolapse into the endocervical canal ("tumor delivery" sign), and greater AP dimension and ET-to-AP ratio compared to EC. These features align with prior studies [8-10, 12] and likely reflect the tumor's invasive growth pattern and stromal involvement. The higher ET-to-AP ratio, in particular, may serve as a surrogate marker for deep myometrial invasion, aiding preoperative risk stratification.

The signal characteristics on T2WI provided particularly valuable discriminative information between UCS and EC. In our study, 90.9% of UCS cases demonstrated markedly heterogeneous T2WI signal intensity, compared to only 30.7% of EC cases (p<0.001). This pronounced heterogeneity in UCS likely reflects its complex histological composition, including areas of hemorrhage, necrosis, and the admixture of carcinomatous and sarcomatous elements [21]. In contrast, EC typically showed more homogeneous intermediate signal intensity on T2WI, consistent with its more uniform glandular architecture [22, 23]. The presence of focal T2-hyperintense regions within UCS tumors often corresponded to cystic degeneration or necrosis at histopathology, while T2-hypointense areas frequently represented densely cellular sarcomatous components or hemorrhage. This striking signal heterogeneity in UCS not only aids in its differentiation from EC but may also correlate with tumor aggressiveness, as areas of necrosis often indicate rapid tumor growth and hypoxia-related treatment resistance.

The heterogeneous enhancement patterns observed in UCS attributable to its

biphasic composition-further distinguish it from EC, which typically exhibits more uniform enhancement due to its epithelial origin. This discrepancy underscores the potential of contrast-enhanced MRI to improve diagnostic specificity. Additionally, DWI revealed higher ADC values in UCS, a finding consistent with its necrotic and cystic components [12, 24]. While Takahashi *et al.* [13] reported similar ADC values between UCS and low-grade EC, our results highlight the importance of integrating ADC with morphological features to reduce diagnostic ambiguity.

Multivariate analysis identified several independent predictors for differentiating UCS from EC, including ill-defined tumor boundaries, heterogeneous T2WI signal intensity, larger tumor volume, and elevated ADC values. The robust performance of our model (AUC=0.935) underscores the value of combining clinical and multiparametric MRI features to enhance diagnostic accuracy. This approach addresses a critical gap in preoperative planning, where misclassification can lead to suboptimal surgical or adjuvant therapy.

The current study has several limitations. The retrospective nature and relatively small sample size may introduce potential biases and limit the generalizability of our findings. Additionally, the exclusive focus on endometrioid adenocarcinoma precludes broader application to other histological subtypes of uterine malignancies. Our analysis was also constrained to conventional MRI parameters, whereas emerging techniques like radiomics could offer more comprehensive diagnostic insights. Notably, we did not evaluate ER-α36 expression, which has been proposed as a valuable diagnostic biomarker in endometrial cancer [25]. These limitations highlight important directions for future research, including expanded patient cohorts encompassing diverse histological subtypes, integration of advanced imaging analytics, and incorporation of molecular marker assessment to enhance diagnostic precision.

In conclusion, our findings demonstrate that UCS exhibits distinct clinical and MRI features that can reliably differentiate it from EC. By integrating these biomarkers into diagnostic algorithms, clinicians can improve preoperative risk assessment and optimize therapeutic decision-making for this aggressive malignancy.

Acknowledgment**:** *We would like to express our gratitude to the Dr. Du and Dr. Hu (pathology departments of the Second Affiliated Hospital of Guangzhou University of Chinese Medicine) for their technical support and assistance in data collection.*

Conflict of interest**:** The authors declare no conflicts of interest related to this study.

Funding**:** This research received no specific grant from funding agencies in the public, commercial, or not-for-profit sectors.

Ethical consideration**:** This study was approved by the Institutional Review Board of the Second Affiliated Hospital of Guangzhou University of Chinese Medicine. Written informed consent was waived due to the retrospective nature of the study, and all patient data were anonymized to ensure confidentiality.

Authors contributions**:** ZQ, contributed to the study concept and design. YH and LW, collected the data.

[DOI: 10.61186/ijrr.24.2.25]

WC and JX, drafted the manuscript. All the authors read and approved the final version of the manuscript.

***AI usage statement*:** No artificial intelligence tools were used in the preparation or writing of this manuscript.

REFERENCES

1. Matsuzaki S, Klar M, Matsuzaki S, Roman LD, Sood AK, Matsuo K (2021) Uterine carcinosarcoma: contemporary clinical summary, molecular updates, and future research opportunity. *Gynecologic Oncology,* ***160****(2): 586-601*.
2. Toboni MD, Crane EK, Brown J, Shushkevich A, Chiang S, Slomovitz BM, *et al.* (2021) Uterine carcinosarcomas: From pathology to practice. *Gynecologic Oncology,* ***162****(1): 235-41*.
3. Travaglino A, Raffone A, Raimondo D, Arciuolo D, Angelico G, Valente M, *et al.* (2022) Prognostic value of the TCGA molecular classification in uterine carcinosarcoma. *Int J Gynecology & Obstetrics,* ***158****(1): 13-20*.
4. Cherniack AD, Shen H, Walter V, Stewart C, Murray BA, Bowlby R, *et al.* (2017) Integrated molecular characterization of uterine carcinosarcoma. *Cancer Cell,* ***31****(3): 411-23*.
5. Matsuo K, Takazawa Y, Ross M, Elishaev E, Podzielinski I, Yunokawa M, *et al.* (2016) Significance of histologic pattern of carcinoma and sarcoma components on survival outcomes of uterine carcinosarcoma. *Annals of Oncology,* ***27****(7): 1257-66*.
6. Ferguson SE, Tornos C, Hummer A, Barakat RR, Soslow RA (2007) Prognostic features of surgical stage I uterine carcinosarcoma. *The American J Surgical Pathology,* ***31****(11):1653-61*.
7. Menczer J (2015) Review of recommended treatment of uterine carcinosarcoma (2015) *Current Treatment Options in Oncology,* ***16:****1-18*.
8. Tanaka YO, Tsunoda H, Minami R, Yoshikawa H, Minami M (2008) Carcinosarcoma of the uterus: MR findings. *Journal of Magnetic Resonance Imaging,* ***28****(2): 434-9*.
9. Huang YT, Huang YL, Ng KK, Lin G (2019) Current status of magnetic resonance imaging in patients with malignant uterine neoplasms: a review. *Korean Journal of Radiology,* ***20****(1): 18-33*.
10. Genever A and Abdi S (2011) Can MRI predict the diagnosis of endometrial carcinosarcoma? *Clinical Radiology,* ***66****(7): 621-4*.
11. Li L, Huang W, Xue K, Feng L, Han Y, Wang R, Gao J (2021) Clinical and imaging features of carcinosarcoma of the uterus and cervix. *Insights into Imaging,* ***12:*** *1-10*.
12. Takeuchi M, Matsuzaki K, Harada M (2016) Carcinosarcoma of the uterus: MRI findings including diffusion-weighted imaging and MR spectroscopy. *Acta Radiologica,* ***57****(10):1277-84*.
13. Takahashi M, Kozawa E, Tanisaka M, Hasegawa K, Yasuda M, Sakai F (2016) Utility of histogram analysis of apparent diffusion coefficient maps obtained using 3.0 T MRI for distinguishing uterine carcinosarcoma from endometrial carcinoma. *J Magnetic Resonance Imaging,* ***43****(6):1301-7*.
14. Huang YT, Chang CB, Yeh CJ, Lin G, Huang HJ, Wang CC, *et al.* (2018) Diagnostic accuracy of 3.0 T diffusion-weighted MRI for patients with uterine carcinosarcoma: Assessment of tumor extent and lymphatic metastasis. *J Magnetic Resonance Imaging,* ***48****(3): 622-31*.
15. Lopez-Garcia MA, Palacios J (eds). Pathologic and molecular features of uterine carcinosarcomas. Semin Diagn Pathol. 2010;27 (3):145–156. Philadelphia: WB Saunders; 2010.
16. Chen X, Arend R, Hamele-Bena D, Tergas AI, Hawver M, Tong GX, *et al.* (2017) Uterine carcinosarcomas: clinical, histopathologic and immunohistochemical characteristics. *Int J Gynecological Pathology,* ***36****(5): 412-9*.
17. Jonson AL, Bliss RL, Truskinovsky A, Judson P, Argenta P, Carson L, *et al.* (2006) Clinical features and outcomes of uterine and ovarian carcinosarcoma. *Gynecologic Oncology,* ***100****(3): 561-4*.
18. Huang GS, Chiu LG, Gebb JS, Gunter MJ, Sukumvanich P, Goldberg GL, *et al.* (2007) Serum CA125 predicts extrauterine disease and survival in uterine carcinosarcoma. *Gynecologic Oncology,* ***107****(3): 513-7*.
19. Ross MS, Chandler CK, Matsuo K, Vargo JA, Elishaev E, Siripong N, *et al.* (2019) Cancer antigen 125 is associated with disease status in uterine carcinosarcoma. *Rare Tumors,* ***11:*** *2036361319884159*.
20. Harano K, Hirakawa A, Yunokawa M, Nakamura T, Satoh T, Nishikawa T, *et al.* (2016) Prognostic factors in patients with uterine carcinosarcoma: a multi-institutional retrospective study from the Japanese Gynecologic Oncology Group. *Int J Clinical Oncology,* ***21****(1):168-76*.
21. Miccò M, Sala E, Lakhman Y, Hricak H, Vargas HA (2015) Imaging Features of Uncommon Gynecologic Cancers. *AJR Am J Roentgenol,* ***205****(6): 1346-59*.
22. Gui B, Lupinelli M, Russo L, Micco M, Avesani G, Panico C, *et al.* (2022) MRI in uterine cancers with uncertain origin: Endometrial or cervical? Radiological point of view with review of the literature. *Eur J Radiol,* ***153****:110357*.
23. Pintican R, Bura V, Zerunian M, Smith J, Addley H, Freeman S, *et al.* (2021) MRI of the endometrium-from normal appearances to rare pathology. *The British J Radiology,* ***94****(1125): 20201347*.
24. Ravishankar P, Smith DA, Avril S, Kikano E, Ramaiya NH (2019) Uterine carcinosarcoma: a primer for radiologists. *Abdominal Radiology,* ***44:*** *2874-85*.
25. Li F, Li L, Li H (2024) Estrogen receptor ER-α36: A diagnostic biomarker for endometrial cancer. *Int J Radiat Res,* ***22****(2): 403-409*.

[DOI: 10.61186/ijrr.24.2.25]